Low-cost laterite-laden household filters for removing arsenic from groundwater in Vietnam and waste management

Thi Hai Nguyen[1], Anh Thao Nguyen[2], Paripurnanda Loganathan[1], Tien Vinh Nguyen[1]*, Saravanamuthu Vigneswaran[1]*, Thi Hoang Ha Nguyen[3], Hai Nguyen Tran[4]

[1] Faculty of Engineering and IT, University of Technology Sydney (UTS), Sydney, Australia
[2] Institute of Environmental Technology, Vietnam Academy of Science and Technology, Hanoi, Vietnam
[3] University of Science, Vietnam National University, Hanoi, Vietnam
[4] Institute of Fundamental and Applied Sciences, Duy Tan University, Ho Chi Minh, Vietnam

Abstract

This study evaluated the performance of a low-cost natural laterite from Thach That (NLTT), Vietnam, for its arsenic (As) removal capacity in a household filter with contaminated groundwater. The NLTT was initially tested in a laboratory column trial lasting 800 h. The breakthrough curves were found to fit the Thomas model very satisfactorily with adsorption capacities of 0.06 and 0.20 mg/g at a flow velocity of 0.85 m/h for the influent As(V) concentrations of 0.1 and 0.5 mg/L, respectively. In household filters at four sites, the median As concentration in groundwaters (0.04–0.19 mg/L) dropped to 0.026–0.054 mg/L after traditional sand filtration. However, after the subsequent NLTT filtration through columns (14 cm inner diameter, 65 cm height) at 0.65 m/h flow velocity, it fell to below the Vietnam and WHO drinking water standard (0.01 mg/L) during seven months of continuous operation. Portland cement and lime were tested as binding agents for the exhausted NLTT waste in a solidification/stabilization process at different ratios. The best ratio of exhausted NLTT: Portland cement: lime for restraining mobility of As from this waste was 3: 1: 0.5. The concrete brick products revealed a suitable compressive strength for using it as building materials in construction work.

Keywords: *Arsenic removal; adsorption; laterite; household filter; solidification/stabilization.*

1. Introduction

Arsenic (As) is a highly toxic element and is released to groundwater by natural processes, including weathering processes (mainly from weathering of sulphide minerals), biological activities, volcanic activities, and/or anthropogenic activities, for example mining activities, leaching of wastes, and wastewaters (Smedley and Kinniburgh, 2002). Long-time exposure to drinking water with contaminated As causes chronic toxicity outcomes for human health, including dermal, nervous, and other body systems (Berg et al., 2001). It is estimated that more than 230 million people in nearly 108 countries worldwide are affected by As contaminated groundwater (Shaji et al., 2020). There are 180 million people throughout South Asia (Bangladesh, India, Pakistan, and Nepal), China, and Southeast Asian countries (Vietnam, Thailand, and Cambodia) facing high risk of As poisoning (Kim et al., 2011; Shaji et al., 2020).

In Vietnam, the majority of its 97 million people live in two deltas, the Red River Delta in the north and the Mekong River Delta in the south of Vietnam, where the groundwater is highly contaminated with As (Agusa et al., 2006; Berg et al., 2001; Glodowska et al., 2021; Nguyen et al., 2020a). The total As concentration in groundwater in the Red River Delta and Mekong River Delta ranged from 0.001–3.05 mg/L (average 0.159 mg/L) and 0.001–0.845 mg/L (average 0.039 mg/L), respectively (Berg et al., 2007). It is estimated that nearly ten million people in the Red River Delta and one million people in the Mekong River Delta are potentially at great risk due to their continual use of As contaminated groundwater.

Numerous water treatment technologies have been devised to remove As from contaminated waters, such as adsorption (Nguyen et al., 2020a), biological treatment (Lievremont et al., 2009), and membrane-related processes (Brandhuber and Amy, 1998). Of these technologies, adsorption is considered to be the best one at a decentralized scale due to its outstanding removal efficiency, simple design, cost-effectiveness, and minimal secondary waste generation. A large number of commercial, synthetic, and natural materials have been used as adsorbents for As removal. Some synthetic nanomaterials, for example, nano iron oxides/hydroxides, nano titanium oxide, nano zerovalent iron, nano copper oxide, nano zinc oxide, and layered double hydroxides were reported to have a high adsorption capacity for As(III) and As(V) in water (Goh et al., 2008; Lata and Samadder, 2016; Pena et al., 2005; Siddiqui and Chaudhry, 2017). However, their practical application in column filters is very limited as their fine powder form can lead to clogging of filters. Other popular commercial adsorbents (i.e., activated carbon and activated alumina) have been identified as highly effective for removing toxic As(III) and As(V) (Kalaruban et al., 2019). However, their prices and regeneration costs are relatively high. This means that their practical application might be restricted in low-income villages. Unlike commercial products, many low-cost natural adsorbents or industrial/agricultural waste products (e.g. clay, goethite, zeolites, laterite, red mud, fly ash, etc.) possess outstanding characteristics, including their local availability, inexpensiveness, and moderately high As removal efficiency (Nguyen et al., 2020a; Nguyen et al., 2009). This has promoted their use as alternative adsorbents for removing As from contaminated water and wastewater (Mohan and Pittman Jr, 2007).

Our previous research found that natural laterite from Thach That district, Hanoi (NLTT), was a promising low-cost adsorbent (US$ 0.10/kg) for removing As from groundwater (Nguyen et al., 2020a). The Langmuir maximum adsorption capacities of NLTT at pH 7 and 30 °C were 0.512 mg/g for As(III) and 0.58 mg/g for As(V), respectively. A community water filtration system packed with this adsorbent was successfully operated in a childcare centre in Ha Nam province, Vietnam, and able to produce safe drinking water (below the Vietnam drinking water As standard of 0.01 mg/L) during 6 months in 2018. However, this filtration system - composed of an aeration tank, a clarifier tank, an adsorption column containing activated carbon and NLTT, and an ultrafilter - is somewhat complicated to use in household filters in rural areas. The purpose of the aeration tank is to oxidize Fe and coprecipitate with As while the clarification tank removes the precipitates. In several Vietnam houses in rural areas, the individual homes are traditionally using only a simple sand filter to remove As, Fe and other contaminants. However, generally only partial removals of these contaminants are achieved with this filter and As in the treated water is mostly higher than the safety level. Therefore, in the first part of this study, a new household filter treatment system packed with NLTT was tested to: firstly, treat the water obtained from the sand filter; and secondly, assess the As removal efficiency at four sites in Vietnam.

One of the problems with using adsorbents to remove As is the disposal of the As containing exhausted adsorbent. Many As waste disposal methods have been applied to prevent the release of toxic As from solid wastes into the environment, which include landfill, mixing with livestock waste, desorption/regeneration, and encapsulation within construction materials (Sullivan et al., 2010). Of these methods, encapsulation through solidification/stabilization (S/S) has received much attention mainly due to its cost-effectiveness, significantly preventing As mobility and generating new building material. The encapsulation technique through S/S process is also identified as the Best Demonstrated Available Technology (BDAT) for hazardous waste disposal by the United States Environmental Protection Agency (USEPA) (Kundu and Gupta, 2008). In this process, normally, As-bearing waste is mixed with some common locally available building materials (e.g. cement, lime, sand, gravel, slag, or polymer) to produce new solidified products. Nguyen et al. (2020b) reported that products made by mixing As-bearing manganese oxides with cement and sand were suitable as building materials in the construction industry. They also reported that As leaching from the encapsulated products was negligible because Ca in the concrete reacted with As to form insoluble Ca arsenate precipitate. This suggestion is tested in the current study by mixing the exhausted adsorbent with cement and lime ($Ca(OH)_2$) at different ratios and measuring As leaching and compressive strength of the encapsulated product to determine its suitability as a construction material. Although a previous study was conducted on mixing exhausted adsorbent with lime, cement and fly ash to determine As leaching behaviour, compressive strength of the mixed-product which is an important property related to its suitability for use as construction material was not reported (Singh and Pant, 2006).

The main objectives of this study were to: (i) evaluate a new low-cost household filter system for removing As from real As contaminated groundwater at four sites in Vietnam; and (ii) determine the efficiency of S/S process on managing the spent adsorbent by mixing it with Portland cement and lime at different ratios. Management of the spent adsorbent was evaluated by measuring As leaching potential and compressing strength of the brick product formed in this mixture.

2. Material and methods

2.1. As adsorbent and chemicals

The natural laterite (NLTT) used in the study was collected at Thach That district, Hanoi City, Vietnam. Dirt and soluble materials adhering to the surface of NLTT were removed by washing with water followed by drying the material at 105 °C inside an oven. The clean and dried NLTT was ground and sieved into particle sizes of 1–2 mm before packing it in the filter column.

All the chemicals and the reagents used in this study were of analytical grade. Stock solution of 1000 mg/L As(V) was prepared by dissolving 4.16 g of sodium arsenate heptahydrate ($Na_2HAsO_4 \cdot 7H_2O$, from BDH Chemical Ltd.) in 1000 mL of deionized water. Feed solutions with As(V) concentrations of 0.10 and 0.50 mg/L were prepared by diluting the stock solution with deionized water. The solution pH was maintained at 7.0 ± 0.1 by adding either nitric acid (0.1M HNO_3) or sodium hydroxide (0.1M NaOH).

2.2. Characterization of NLTT

The NLTT properties were described in detail in our recent study (Nguyen et al., 2020a). To concisely summarize them, the NLTT was composed of the minerals. goethite, hematite, nacrite, quartz, and anatase. The main chemical composition of NLTT was Fe_2O_3 (48.7%), Al_2O_3 (18.2%), SiO_2 (14.0%), and TiO_2 (2.89%), which could facilitate As adsorption. These oxides have been reported to have removed As from contaminated water by complexation reactions/inner sphere coordination via ligand exchange process (Cheng et al., 2019; Mohan and Pittman Jr, 2007; Nguyen et al., 2020c; Pena et al., 2005; Siddiqui and Chaudhry, 2017; Zhao et al., 2018).

The characteristics of NLTT before and after As adsorption were examined to understand the adsorption mechanisms. The mineral composition and main functional groups of NLTT were examined using X-ray Diffraction (XRD; Empyrean-PANalytical) and Fourier transform infrared spectroscopy (FTIR; Nicolet iS5), respectively.

2.3. Laboratory column adsorption study

Batch adsorption of As on NLTT was previously studied with artificially contaminated feeding solutions, and the Langmuir maximum adsorption capacities of this adsorbent at pH 7 and 30 °C were found to be 0.512 mg/g for As(III) and 0.58 mg/g for As(V), respectively (Nguyen et al., 2020a). In our previous study these adsorption capacities were compared with those of many other low-cost adsorbents reported in literature in treating As(III) or As(V) at realistic concentrations (0.1–0.5 mg/L) and they were found to be similar to or higher than the others (Nguyen et al., 2020a). For example, Glocheux et al. (2013) showed that adsorption capacities of raw laterite towards As(V) and As (III) were 0.301 and 0.128 mg/g, respectively, which are lower than with those of NLTT. However, no column adsorption experiments were reported for this adsorbent. Column adsorption experiments provide information on the dynamics of As adsorption behaviour compared to the static batch adsorption experiment.

Consequently, they give practical information for NLTT application on continuous As removal in real treatment plants. Therefore, before setting up the household filters in the field, a laboratory experiment was conducted to comprehend As adsorption behaviour of NLTT in a column set-up.

The column adsorption study was conducted using a glass column of 30 mm inner diameter and 0.50 m height. The feed solution containing two As(V) concentrations (0.1 and 0.5 mg/L) was pumped in an up-flow mode through the column at a constant flow rate of 10 mL/min (0.85 m/h) using dosing pumps (Master flex L/S). The column was packed with 440 g NLTT (corresponding to 0.41 m bed-height). To prevent any migration of the NLTT from the packed column and to allow uniform distribution of the solution through the column, 1.0 mm acrylic beads and cotton balls were placed at the top and bottom of the columns. Figure 1 shows a schematic diagram of laboratory column study.

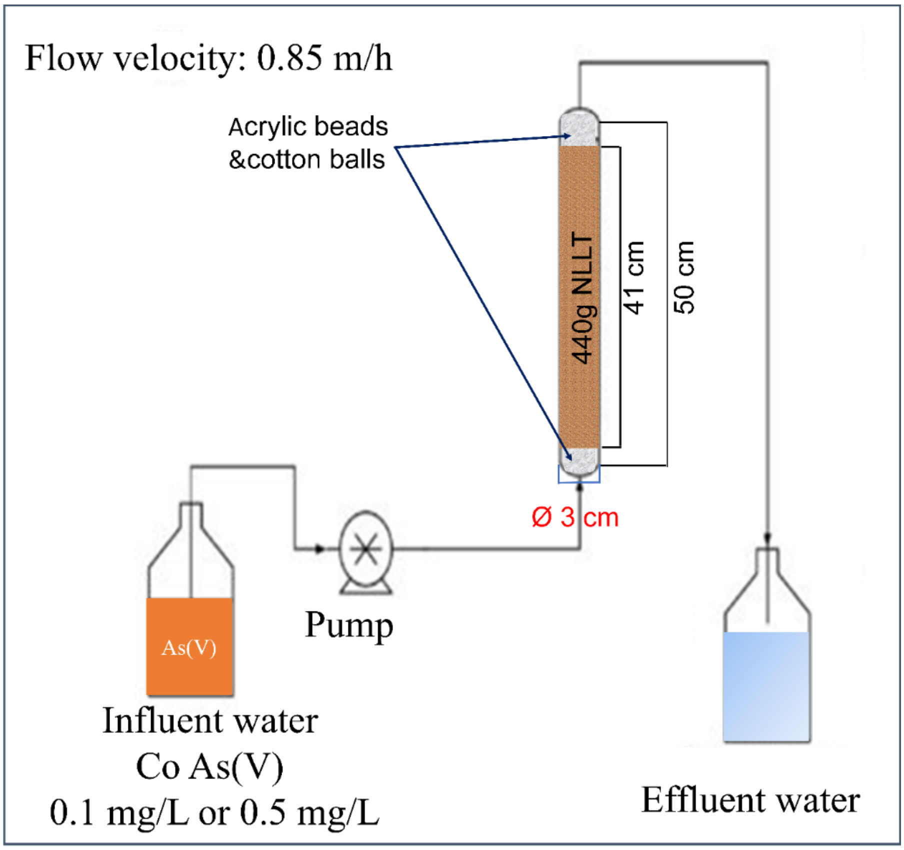

Figure 1. Schematic diagram of laboratory column study

Samples were collected every 2 h on the first day, then once daily over the first 3 weeks, followed by 2–3 samples weekly until the As(V) concentration in the effluent approached the initial concentration (time of column saturation with As(V)). The samples were filtered using 0.45 µm filters, and filtrates were analysed for As using the method described in the next section.

2.4. As analysis

The As concentration in the water samples was determined by an inductively coupled plasma mass spectrometry (ICP-MS, NexION 2000, US). In order to minimize spectral interferences (including polyatomic ion $^{40}Ar^{35}Cl^{+}$ interference) hampering As determination, the dynamic reaction cell (DRC) mode ultilising oxygen as reaction gas was used. The monitored ions in this method were $^{75}As^{16}O^{+}$ (m/z 91). Peak hoping measurement mode was adopted. An internal calibration curve (^{115}In) with a correlation coefficient of 0.999941 was used to determine the As concentrations in the water samples. This calibration graph was linear in the range of 1.000–50.000 µg/L. Average of five readings were taken. The limits of detection and quantifications were 0.0005 and 0.0017 µg/L, respectively.

2.5. Field study with household filter

The household filter system had a filter cartridge packed with 15 kg NLTT (particle size of 1–2 mm) and 1 kg of sand, as shown in Figure 2. The sand was placed at the bottom of the filter cartridge, and NLTT media was then placed above the sand layer. The filter cartridge was prepared from a PVC water pipe with an inner diameter of 14 cm and 65 cm height. Four such filters were installed, two in Hoang Tay commune, Kim Bang district, Ha Nam province, and two in Phuong Tu commune, Ung Hoa district, Hanoi, Vietnam. Groundwaters that were pretreated with traditional sand filters were passed through the NLTT filter at a filtration rate of 10 L/h (0.65 m/h).

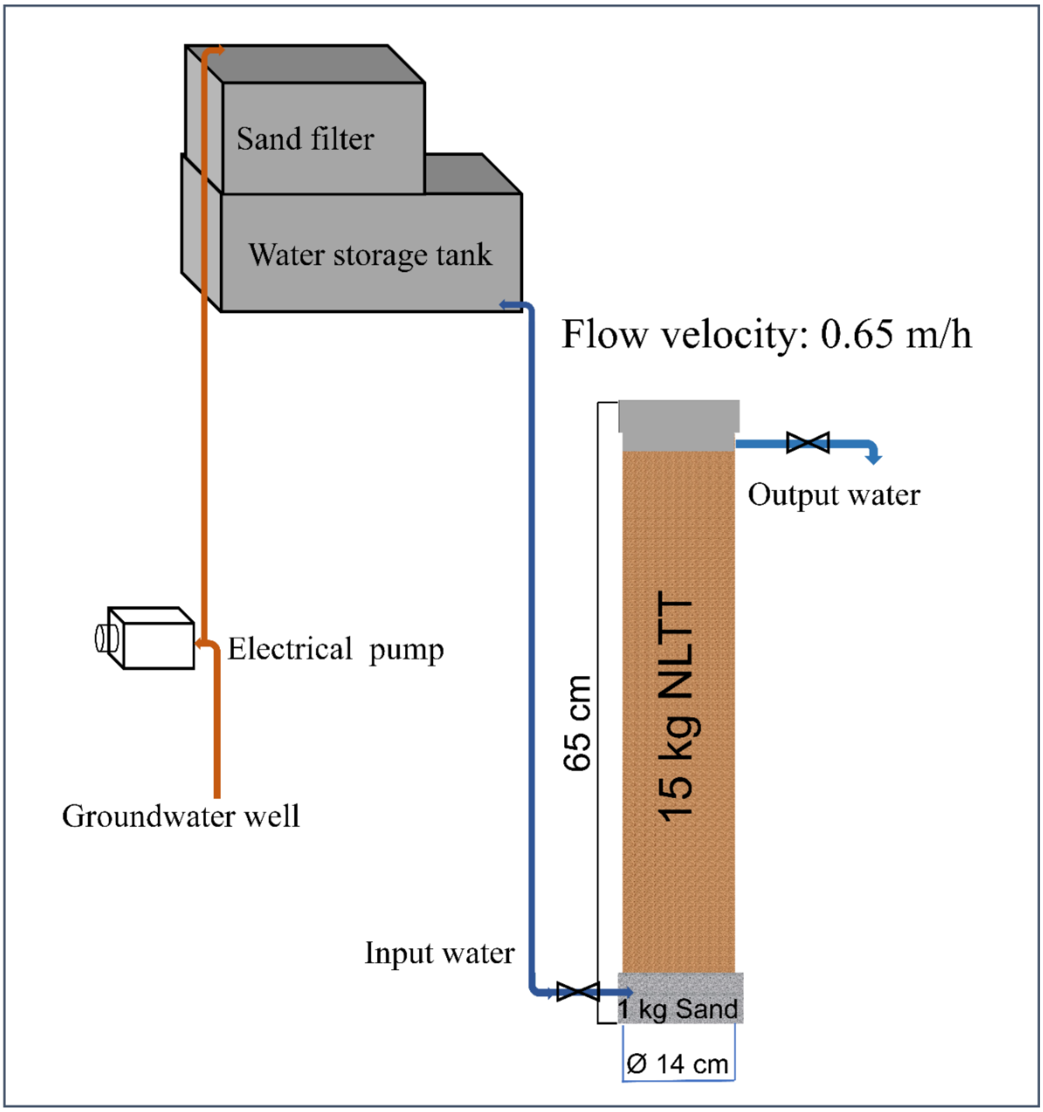

Figure 2. Schematic diagram of household filter system

Groundwater samples before and after treatment by (i) the traditional sand filters and (ii) NLTT filter system were collected fortnightly over 7 months. The sand filter, which has been traditionally used in Vietnam, was made up of two main containers: sand filter tank (1 m × 0.8 m × 0.7 m) and water storage tank (1 m × 1.2 m × 1 m). Sand filter tank was constructed above a water storage tank and filled with locally available sand (approximate 300 kg). The groundwater is pumped from the tube well into the sand filter tank and allowed to trickle through the sand layers into the water storage tank. The samples were filtered using 0.45 µm filters, and filtrates were analyzed for As using ICPMS and Fe using an Atomic Absorption Spectrometer (PinAAcle 900T, USA). The As-laden NLTT adsorbent samples at the second household (H2) in Hoang Tay commune were collected and characterized after three months and six months' operation. At each collection time, two As-laden NLTT adsorbent samples were collected, one from the bottom layer (approximately 55 cm from the lip of the filter column) and the other one from the top layer (approximately 10 cm from the lip of the filter column).

2.6. Solidification/stabilization

An analysis of the management of exhausted NLTT was carried out using the solidification/stabilization method. Schematic diagram of solidification/stabilization study is shown in Figure 3. The exhausted NLTT media was prepared by soaking 5 kg NLTT material into 5 L of synthetic As(V) solutions of 4.5 g/L concentration. After 40 days soaking, the solid phase (adsorbent containing adsorbed As(V)) of the mixture was separated by filtration, dried in an oven for 48 h at 50 °C, and stored in tightly closed bags for later use in the solidification/stabilization process.

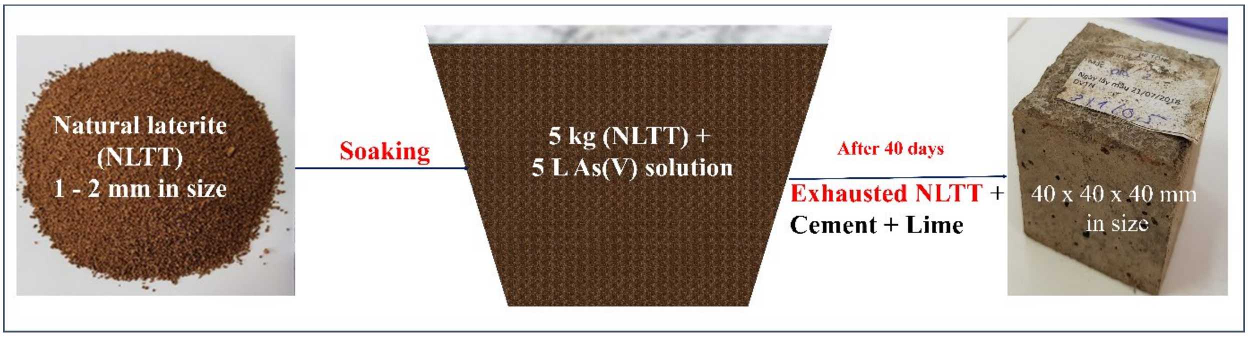

Figure 3. Schematic diagram of solidification/stabilization study

0.15 g of NLTT samples containing the adsorbed As(V) were digested in an acid solution made by a mixture of 2 mL concentrated HNO_3, 4 mL concentrated HCl, and 2 mL concentrated

HF using a microwave digester for 3 h. The digested solutions were diluted to an appropriate volume and the As concentration was determined. Results showed that the digested NLTT had 0.564 mg/g NLTT for As(V). This value is approximately the same as the Langmuir maximum adsorption capacity of 0.58 mg/g for As(V) at pH 7 and 30 °C reported for NLTT (Nguyen et al., 2020a). This confirms that 40 days soaking of NLTT in 4.5 g/L As(V) solution had completely saturated the adsorption sites of NLTT with As(V). Therefore, the adsorbent material prepared by this method can be used as a material representing exhausted adsorbent.

2.6.1. Preparation of concrete bricks

Three different concrete brick products, namely NLTT3C1L0, NLTT3C1L1, and NLTT3C1L0.5, were prepared by mixing exhausted NLTT, Portland cement (C), and lime (L) at NLTT : C : L mass ratios of 3:1:0, 3:1:1, and 3:1:0.5, respectively. Portland cement and lime used in the mixture were purchased from a local construction material store. Initially, 1.8 kg of exhausted NLTT adsorbent was mixed with 0.5 L of deionized water, and then cement and lime were added to this mixture at the specified ratios. Then, the composite materials were thoroughly mixed using a laboratory concrete mixer. The mixed slurries were cured by placing them inside 40 × 40 × 40 mm cement cube moulds for 24 hours, as shown in Figure 3. The concrete bricks formed were taken out from the moulds and soaked in water for 27 days before conducting tests on them.

2.6.2 Leaching test

To determine the amount of As leaching to the environment from the concrete brick samples, a leaching test was conducted on all concrete samples. In this test, the concrete bricks samples with sizes of 40 × 40 × 40 mm were cut into smaller ones of 20 × 20 × 20 mm size with weights of approximately 75 g each. These small concrete bricks were then washed with deionized (DI) water to eliminate any adhering dirt before placing them inside closed vessels without agitation that contained different leachants, such as distilled water (DW), 0.1 M HNO_3, and 0.1 M NaOH (Kundu and Gupta, 2008).

2.6.3. Physical properties of concrete bricks

The compressive strength property of the final concrete brick samples was determined using Vietnam standard methods, namely the Brick test method (TCVN 6355:2-2009). The compressive strength of concrete brick samples was measured using a concrete compressor TYA-300 LUDA.

3. Results and discussion

3.1. Laboratory column adsorption study

The effect of initial As(V) concentration (Co = 0.1 mg/L and 0.5 mg/L) on the adsorption capacity of NLTT towards As(V) was investigated.

As seen in Figure 4, the breakthrough curves had a typically smooth S shape, indicating that the adsorption was controlled by the length of the mass transfer zone. Results also show that the initial concentration had a strong effect on the shape and gradient of the breakthrough curves. The breakthrough curve of NLTT for the initial As(V) concentration of 0.5 mg/L was steeper than that of initial As(V) concentration of 0.1 mg/L. This outcome is consistent with previous studies on As(V) removal by adsorbents in column experiments (Brion-Roby et al., 2018; Yunnen et al., 2017). Yunnen et al. (2017) reported that the breakthrough curves for As(V) adsorption in columns containing organically modified plant grains at higher As(V) concentration were sharper due to a relatively smaller mass transfer zone and a more intra-particle diffusion-controlled process. Moreover, at a higher initial concentration of As(V), the larger amount of As(V) passing through the column per unit time resulted in smaller mass transfer resistance, higher driving force, and an earlier saturation (Brion-Roby et al., 2018; Yunnen et al., 2017).

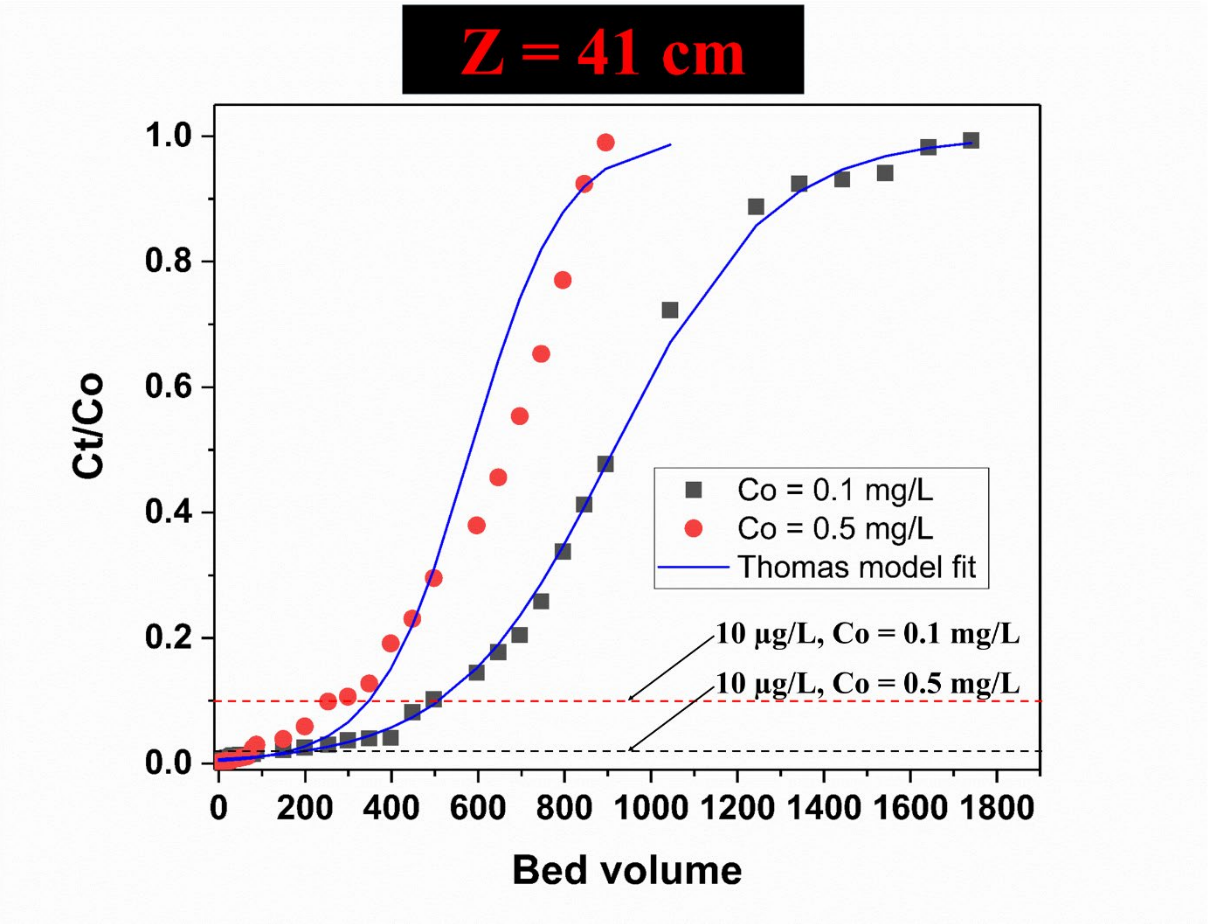

Figure 4. Breakthrough curves for As(V) adsorption on NLTT at two feed concentrations (Experimental conditions: Co: 0.1 mg/L and 0.5 mg/L; Bed height Z: 41 cm; flow velocity 0.85 m/h; pH: 7.0; room temperature)

The Thomas model (Thomas, 1944) was used to describe the breakthrough curves. This model is the most popular and widely applied in column adsorption studies (Eeshwarasinghe et al., 2018; Nur et al., 2015). Furthermore, it accurately describes the column adsorption capacity unlike many others. The nonlinear and linear forms of the Thomas model are described in Equations (1) and (2), respectively:

$$\frac{C_t}{C_0} = \frac{1}{1 + \exp(k_{TH} q_{TH} \frac{m}{Q} - k_{TH} C_0 t)} \quad \textbf{(1)}$$

$$\ln\left(\frac{C_0}{C_t}-1\right) = K_{TH}q_{TH}\frac{m}{Q} - k_{TH}C_0 t \qquad \textbf{(2)}$$

where k_{TH} is the Thomas adsorption rate constant (L/h.mg), q_{TH} is the maximum column As(V) adsorption capacity (mg/g), Co is the inlet As(V) concentration (mg/L), Ct is the outlet As(V) concentration at time t (mg/L), m is the mass of adsorbent (g), Q is the volumetric flow rate (L/h), and t is the filtration time (h). The values of k_{TH} and q_{TH} were determined from the linear plot of $\ln\left(\frac{C_0}{C_t}-1\right)$ against t and are presented in Table 1. The model satisfactorily described the As(V) breakthrough in the column at the two inlet concentrations (0.1 and 0.5 mg/L) tested as indicated by the high coefficient of determination values (R^2) (0.95, 0.98) (Table 1, Figure 4).

Table 1. Thomas model parameters for As(V) adsorption on NLTT

Co	***q_{exp}***	**Thomas model parameters**		
(mg/L)	***(mg/g)***	***k_{TH}*** (L/h.mg)	***q_{TH}*** (mg/g)	***R^2***
0.1	0.05	0.117	0.058	0.98
0.5	0.20	0.038	0.198	0.95

The results show that the adsorption capacity increased from 0.058 to 0.198 mg/g, and the kinetic coefficient, K_{TH}, decreased from 0.117 to 0.038 L/h.mg as the initial As(V) concentration rose from 0.1 mg/L to 0.5 mg/L, respectively (Table 1). The higher values of q_{TH} at higher initial As(V) concentration is due to the higher driving force for adsorption of As(V) on NLTT. This result agrees with previous studies (Abdolali et al., 2017; Nguyen et al., 2015). The Thomas adsorption capacities of NLTT are much lower than the Langmuir maximum adsorption capacity of NLTT for As(V) (q_{max} = 0.580 mg/g) obtained in a static batch study (Nguyen et al., 2020a) because the equilibrium As(V) concentration (> 10 mg/L) at the calculated Langmuir maximum adsorption value was much higher than the inlet As(V) concentrations used in the column experiment (0.1 and 0.5 mg/L). However, the adsorption capacities in the batch adsorption study at similar As(V) concentrations in solution phase of 0.25 mg/L and 0.5 mg/L as in the column study were 0.020 mg/g and 0.037 mg/g, respectively (Nguyen et al., 2020a). These results show that the adsorption capacities in batch adsorption process are lower than the Thomas adsorption capacities obtained in the column adsorption study at comparable solution As(V) concentrations. The reason for the higher values in column study is that the driving force for adsorption is maintained always constant due to the continuous mode of feeding the As(V) solution to the adsorbent fixed bed, whereas in the batch experiment the driving force diminishes progressively with time due to the removal of the As(V) from the solution by adsorption.

Table 2. Comparison of Thomas adsorption capacities obtained in the current study with those reported in other studies.

Adsorbent	As (V) concentration (mg/L)	Flow rate (L/h)	Thomas adsorption capacity (mg/g)	References
NLTT	0.5	0.6	**0.198**	**This study**
Manganese oxide ore	0.25	0.15	0.151	(Nguyen et al., 2020b)
Multi walled carbon nanotubes	0.04	1.20	0.014	(Ali, 2018)
Natural pozzolan	0.40	0.24	0.003	(Kofa et al., 2015)
Thioglycolated sugarcane carbon	1.50	0.18	0.083	(Roy et al., 2013)
Rice husk	0.015	0.42	0.103	(Asif and Chen, 2017)
Iron mixed mesoporous pellet	0.5	1.23	0.099	(Te et al., 2018)

Table 2 summarizes a comparison of the Thomas adsorption capacities obtained for NLTT in this study with those reported for other adsorbents. The data indicate that NLTT possessed a higher adsorption capacity than many natural adsorbents (manganese oxide ore, rice husk, and natural pozzolan) and synthesized adsorbents (multi-walled carbon nanotubes, thioglycolated sugarcane carbon, and iron mixed mesoporous pellet).

3.2. Field studies

3.2.1. NLTT mineralogy and functional groups changes after As adsorption

The mineralogy of NLTT before and after adsorption in field filters was determined using X-Ray powder diffraction. Figure 5 shows five different XRD patterns: (1) pristine NLTT; (2) As-laden NLTT at the top layer (approximately 10 cm from the lip of the filter column) after three months; (3) As-laden NLTT at the bottom layer (approximately 55 cm from the lip of the filter column) after three months; (4) As-laden NLTT at the top layer after six months; and (5) As-laden NLTT at the bottom layer after six months. The peaks for the main component minerals such as goethite (FeOOH), hematite (Fe_2O_3), nacrite ($AlSiO_5(OH)_4$), quartz (SiO_4), and anatase (TiO_2) of NLTT adsorbent after the field test appeared again after adsorption. However, the peak intensities of goethite, hematite, and nacrite of As-laden NLTT after three months and six months were slightly reduced from that of pristine NLTT. The peak intensity of As-laden NLTT at the bottom layer was lower than that of As-laden NLTT at the top layer after three months.

The same trend was also observed for the two layers after six months. The reduction in peak intensity of the minerals is probably due to As(V) reacting with Fe oxide/hydroxide sites in goethite and hematite and Al oxide/hydroxide sites in nacrite, slightly altering these minerals' crystal structures. The adsorbent at the bottom layer had lower peak intensities than that at the top layer. This is because the filter system was operated in the up-flow mode (solution moving from bottom of the column to top). In this mode of operation the NLTT adsorbent at the bottom layer would have had contact with water containing a higher As concentration than that at the top layer, because by the time the water reached the top layer some of the As in the water would have been removed by the bottom layer. Moreover, the XRD patterns of NLTT after six months (Figure 5 - [4] and [5]) possess a clear peak intensity change from those of NLTT after three months due to NLTT interacting with a larger amount of As that passed through the column during the longer period of time (Rout et al., 2015).

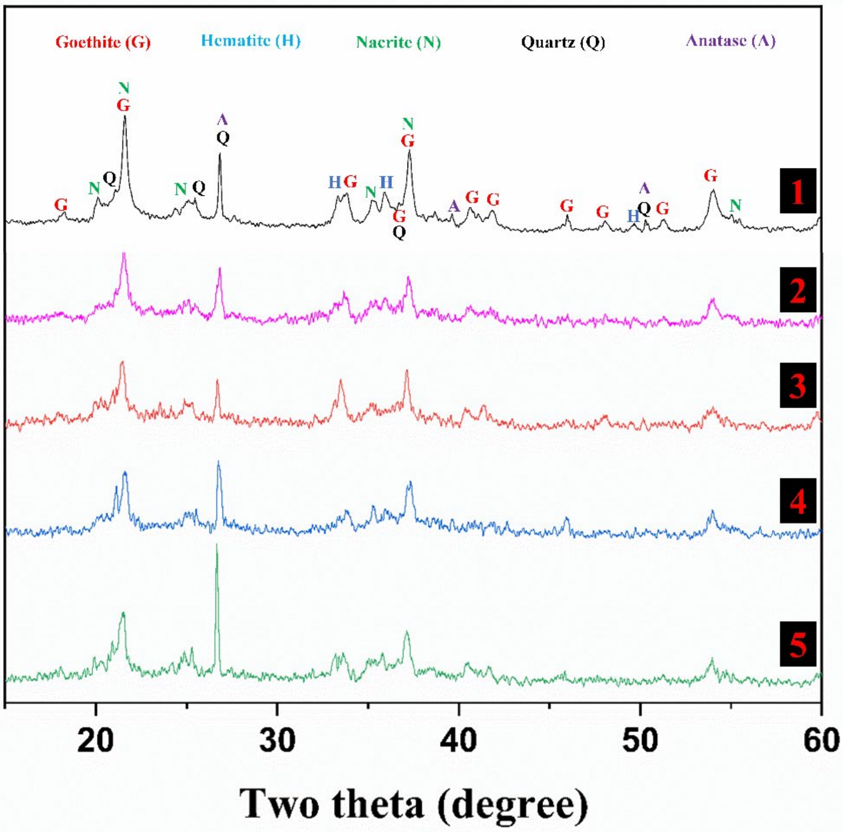

Figure 5. XRD pattern of (1) pristine NLTT; (2) As-laden NLTT at the top layer after 3 months, (3) As-laden NLTT at the bottom layer after 3 months, (4) As-laden NLTT at the top layer after 6 months, and (5) As-laden NLTT at the bottom layer after 6 months

The main functional groups on the surface of the pristine NLTT, and As-laden NLTT at the top and bottom layers at 3 months and 6 months after adsorption were determined by FTIR.

Figure 6 shows that the surfaces of all As-laden NLTT possess similar main functional groups, such as Si–O–Fe (at approximately 1100 cm^{-1}), Si–O (at 1030 cm^{-1}), Al–OH (at 910 cm^{-1}), Fe–OH (at 798 cm^{-1}), Fe–O (at 460 cm^{-1}), and -O-H (at the region of 3730 cm^{-1} and 3100 cm^{-1}) as those of pristine NLTT. Additionally, the results show there was no change in the intensities of FTIR spectra of As-laden NLTT after three months operation compared to that of pristine NLTT adsorbent. On the other hand, the FTIR spectrum of As-laden NLTT after six months of operation (Figure 6 – (4) and (5)) shows there was a remarkable decline in absorbance for all the main functional groups. This is due to the longer period of interaction between As and NLTT leading to larger amounts of As adsorption. Both the XRD and FTIR data showed that As was adsorbed onto the Fe and Al containing minerals in NLTT, and the amount adsorbed was higher at the bottom layer and at the longer operation time.

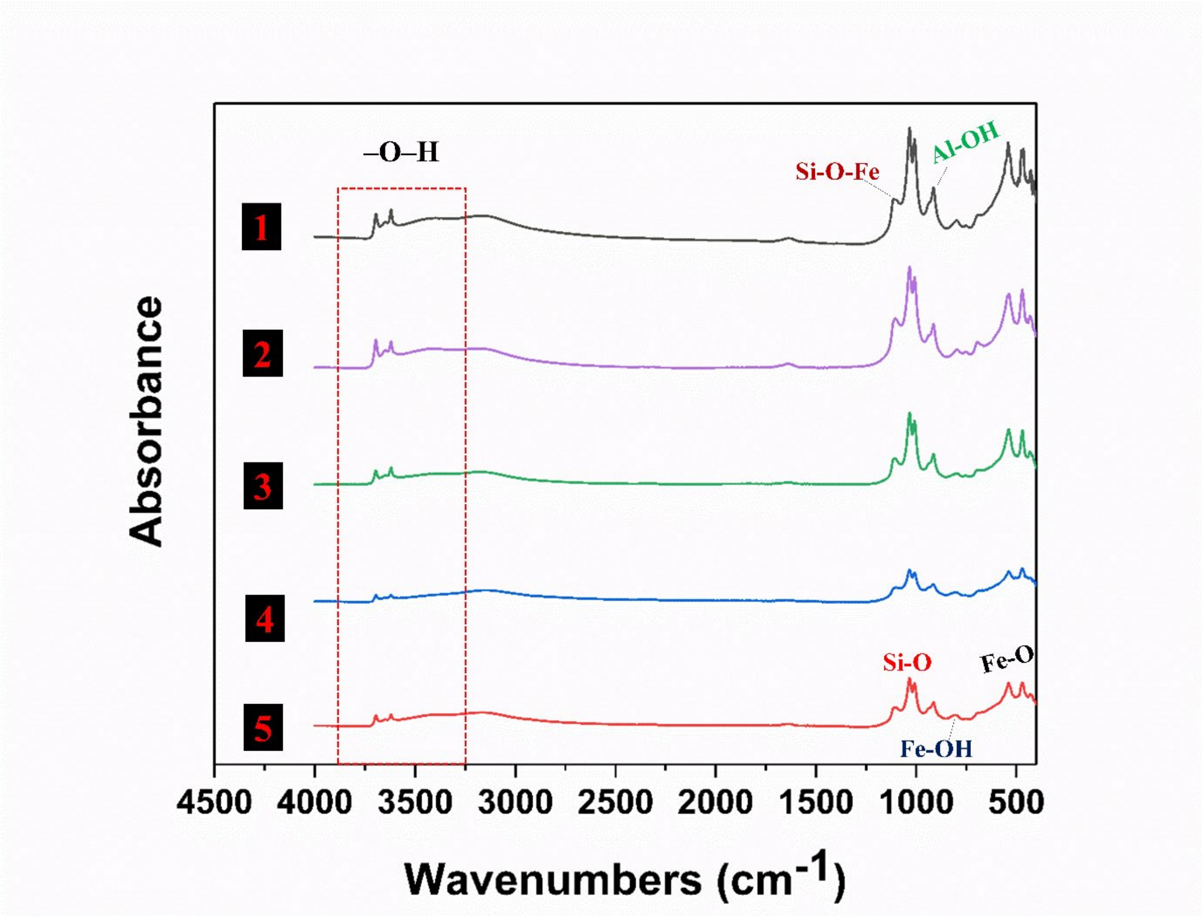

Figure 6. FTIR spectrum of (1) pristine NLTT; (2) As-laden NLTT at the top layer after 3 months, (3) As-laden NLTT at the bottom layer after 3 months, (4) As-laden NLTT at the top layer after 6 months, and (5) As-laden NLTT at the bottom layer after 6 months.

3.2.2. Performance of NLTT filter system

Figure 7 presents the NLTT filter effectiveness in removing As in four different households - H1, H2, H3, and H4 (H1 and H2: two households in Hoang Tay commune; H3 and H4: two households in Phuong Tu commune). Over the seven months of operation in Hoang Tay commune (May 2019 to January 2020), the results show that the total As concentration (mg/L) in groundwater feed to filters in H1 and H2 houses ranged from 0.156 to 0.235 (median 0.19) and 0.114 to 0.17 (median 0.15), respectively. The disparity in total As concentration in the two households is probably due to spatial hydrological and geochemical differences between the locations of the households. Such differences even within short distances apart in Vietnam were reported by Berg et al. (2007).

During the 6 months operation (September 2020 to February 2021) in Phuong Tu commune, the total As concentration in groundwater (mg/L) in H3 and H4 houses ranged from 0.047 to 0.056 (median 0.052), and 0.027 to 0.05 (median 0.040), respectively. The total As concentrations in groundwater in the two households in this commune were much lower with reduced variability compared to those in the two households in Hoang Tay commune.

As evidently seen in Figure 7, the concentration of total As passing through the sand filter had decreased considerably. However, they were still 2.6 to 5.4 times higher than that of the Vietnamese drinking water standard and WHO guideline (0.01 mg/L). Therefore, it is necessary to apply another household filter that can provide safe and sustainable drinking water at a decentralized scale.

To reduce As concentration further, the sand filter treated water was passed through the NLTT filter system. The results show that total As concentration in the output water in the H1 and H2 households ranged from 0.004 to 0.009 mg/L (median 0.006 mg/L) and 0.003 to 0.01 mg/L (median 0.0066 mg/L), respectively. The average As removal efficiency was 88%. The total As concentration in the output water in the H3 and H4 households ranged from 0.0004 to 0.009 mg/L and 0.0004 to 0.003 mg/L, respectively. The average As removal efficiency in these two household filters was 92%.

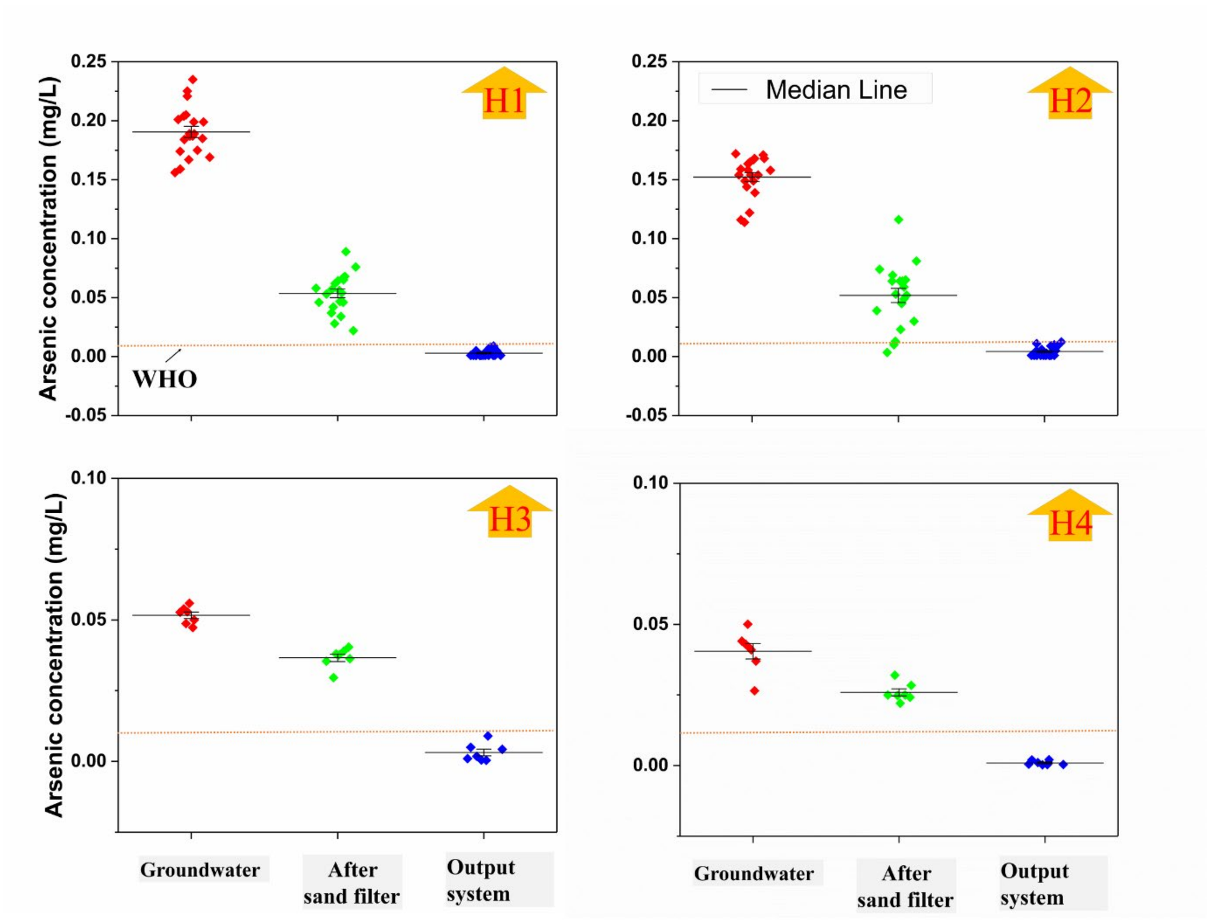

Figure 7. As concentration in groundwater (red dots), after sand filter (green dots), and in the output of NLTT filters (blue dots). The horizontal line in each graph represents the World Health Organization (WHO) As concentration limit (0.010 mg/L).

Modelling of the data from the household filter system could not be conducted because generally all values for Ct/Co were less than 0.1. This is due to the low influent As concentrations that entered the NLTT column (0.02–0.05 mg/L compared to 0.1 and 0.5 mg/L used in the laboratory column study) and adsorption of very high proportion of the As that entered. As a result of this, significant breakthrough of As has not occurred. There was also high variability in the influent concentration because the pre-treatment of the water with sand filter removed variable amounts of As.

The average Fe concentrations in the H1 and H2 households' effluents were 0.13 mg/L and 0.167 mg/L, respectively. The output filtered water in the H3 and H4 households had a much smaller concentration of Fe (0.05 mg/L). The range of Mn concentration in the treated water in all households was 0.17–0.24 mg/L. Both the concentrations of Fe and Mn were below the Vietnamese drinking water quality standard (QCVN 01:2009/BYT) (0.3 mg/L for both of Fe and Mn). During the 7 months operation of the filters, at each household, a total of approximately 2.1 m^3 water was treated to produce safe drinking water (As concentration below the Vietnam and WHO drinking water standard of 0.01 mg/L). The cost of treating 1 m^3 water using NLTT is estimated to be lower than US$ 0.71/m^3 ((US$ 0.1/1 kg NLTT × 15 kg)/2.1 m^3).

3.2.3. Mechanisms of As removal by the filters

In this study, the existing household sand filters were utilized as a beneficial pre-treatment step to enhance the removal efficiency and extend the lifetime of the new household-scale NLTT treatment system. According to Nitzsche et al. (2015), sand filter plays an important role in the efficient removal of As, Fe, and Mn in groundwater. Apart from the enhanced removal of As by the sand filters presented in Figure 7, the average of Fe concentration (mg/L) after sand filtration in the four households (H1, H2, H3, and H4) also dropped significantly, from 10.3 to 0.39, 9.76 to 0.17, 1.44 to 0.036, and 0.914 to 0.030, respectively. Moreover, the average Fe/As ratio in the effluents of sand filters of the four households also fell to 7.3, 11, 1.0, and 1.2, respectively, which are much lower than the respective influent concentration ratios (Figure 8). The simultaneous decrease in the total As concentration, iron concentration, and the Fe/As ratio can be explained by the co-precipitation mechanism of Fe and As in water. This mechanism was discussed in detail in our previous study (Nguyen et al., 2020a). Briefly, when groundwater containing soluble Fe^{2+} and As(III) was pumped into the sand filter tank containing natural air, these ions were oxidized to insoluble Fe^{3+} and As(V) and coprecipitated. The co-precipitation process resulted in the formation of $FeAsO_4.2H_2O$ and $Fe_3(AsO_4)_2.8H_2O$ precipitates. Thus, a major portion of both Fe and As was removed from the water.

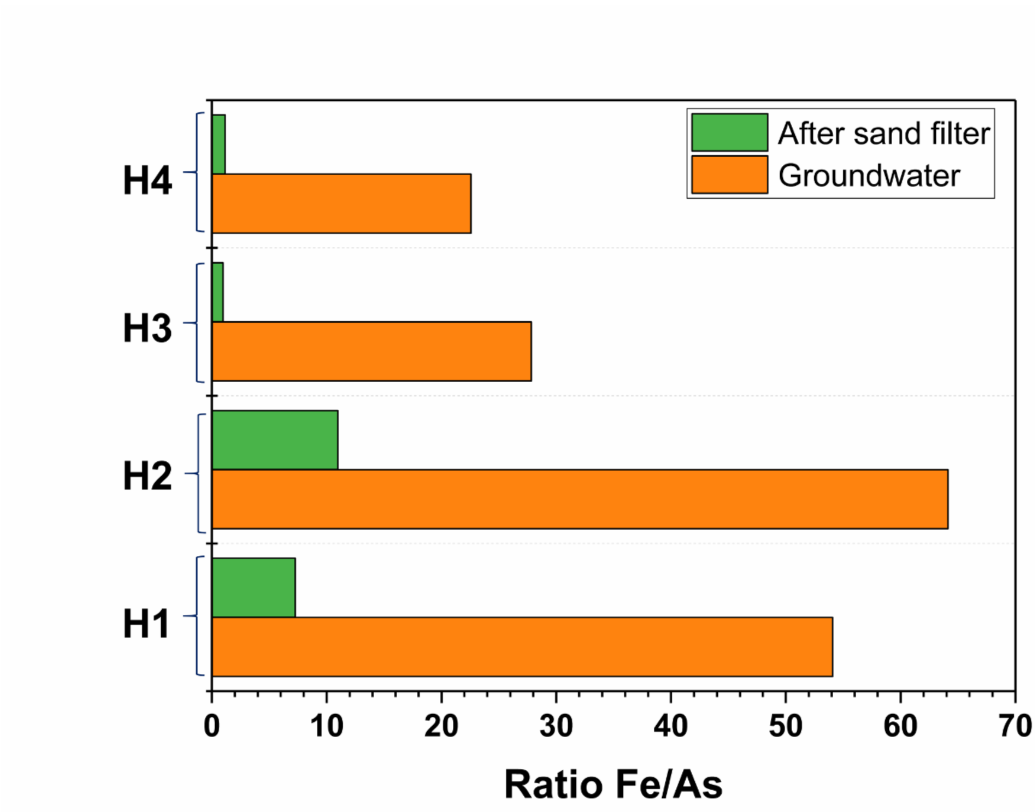

Figure 8. Ratio of Fe/As in ground water, after sand filtration in the four households.

Meng and Korfiatis (2001) reported that an Fe/As ratio ≥ 40 was needed to effectively remove As from groundwater by co-precipitation. The average Fe/As ratio in groundwater of the H1 and H2 households were 54 and 64, respectively, which were higher than that of H3 and H4 households of 27 and 24, respectively (Figure 8). The higher percentage removal of As by sand filters in H1 and H2 households (Figure 7) than in H3 and H4 households is due to the higher Fe/As ratio in the groundwaters of H1 and H2 households.

When the sand filter treated water was passed through the NLTT filter, most of the remaining As in the form of As(V) in the water was removed by adsorption on the Fe and Al oxides/hydroxides in the laterite by inner-sphere complexation as explained by others (Kalaruban et al., 2019; Mohan and Pittman Jr, 2007; Nguyen et al., 2020a). The reactions are represented by the following equations:

$$-\mathbf{X}\mathrm{OH} + \mathrm{As(V)}^{-} \rightarrow -\mathbf{X}\mathrm{As(V)} + \mathrm{OH}^{-} \quad \textbf{(3)}$$

$$-\mathbf{X}\mathrm{OH} + \mathrm{As(V)}^{2-} \rightarrow -\mathbf{X}\mathrm{As(V)}^{-} + \mathrm{OH}^{-} \quad \textbf{(4)}$$

where X represents Fe in goethite/hematite or Al in nacrite, and $As(V)^-$ and $As(V)^{2-}$ represent $H_2AsO_4^-$ and $HAsO_4^{2-}$, respectively. Both these species of As(V) are present at the neutral pH of the ground waters. At slightly lower pH, the monovalent species predominates and at slightly higher pH, the divalent species predominates.

3.3. Solidification/Stabilization

3.3.1. Compressive strength of concrete bricks made from spent adsorbent

The compressive strength of NLTT3C1L0 (20.67 MPa) was higher than that of the other two concrete bricks, NLTT3C1L0.5 (15.30 MPa), and NLTT3C1L1 (18.27 MPa). The results suggested that adding lime materials into concrete components could slightly undermine the bricks' compressive strength. According to the Vietnam concrete bricks and interlocking concrete bricks standard (TCVN 6477:2016), the compressive strength of concrete products should be in the 3.5 MPa to 20 MPa range. Concrete bricks are commonly used in construction work. According to the British concrete standard (BS 8500: 2002, Part 1 and 2), concrete with the compressive strength of 10–20 MPa, can be used for non-structural works such as patio slabs and pathways (10MPa), pavement kerbs, and floor blinding (15MPa), and international floor slabs, flooring for the workshops, garages, and driveways (20MPa). Therefore, all three concrete products created in this study can be used for pavement kerbs, garages, and driveways, which have limited contact times with people.

3.3.2. As leaching from concrete bricks

The concentration of As leached from concrete products in three different leachates (0.1 M NaOH, distilled water, and 0.1 M HNO_3) at different leaching times is presented in Figure 9. The results indicate that strong alkaline and acid conditions could lead to significant leaching of As from the concrete mixtures. In general, the As leachability from all three concrete bricks followed the order of 0.1 M NaOH > 0.1 M HNO_3 > distilled water. As concentration increased rapidly during the first seven days and then slowly in the next 35 days. A similar trend was reported in other studies (Kundu and Gupta, 2008; Singh and Pant, 2006). In all three leachates, the highest concentration of As in the leachate was observed from the NLTT3C1L1 sample. The lowest leaching was observed for NLTT3C1L0.5 in acid and distilled water environments and for NLTT3C1L0 in a strong alkaline environment. The maximum As concentrations in the 0.1 M NaOH leachate from NLTT3C1L1, NLTT3C1L0.5, and NLTT3C1L0 were 1.705 mg/L, 0.993 mg/L, and 0.54 mg/L, respectively. The corresponding concentrations from 0.1 M HNO_3 leachant were 0.0632 mg/L, 0.0362 mg/L, and 0.0511 mg/L, respectively. Notably, the As concentrations in the leachates from the samples using distilled water were extremely low. These data show that the total As concentration in the leachates from all three solidified/stabilized products using all three leachants was well below the recommended limit of 5 mg/L stipulated in the TCLP of USEPA (Jing et al., 2005) .Of the three products, the one with the higher rate of lime addition had the highest As leached by all three leachants. Kundu and Gupta (2008) also reported that when a large amount of lime was added to concrete, As leaching increased because of higher diffusivity of As through the concrete matrix. Taking these results into account, NLTT3C1L0.5 and NLTT3C1L0 appear to be the best products able to prevent As leaching into the environment. For the As leaching with distilled water and acid leachant, the pH conditions generally prevalent in most environments, NLTT3C1L0.5 produced less leaching than NLTT3C1L0. Therefore, adding lime to cement at this ratio is recommended for mixing with the exhausted adsorbent before disposing of this waste.

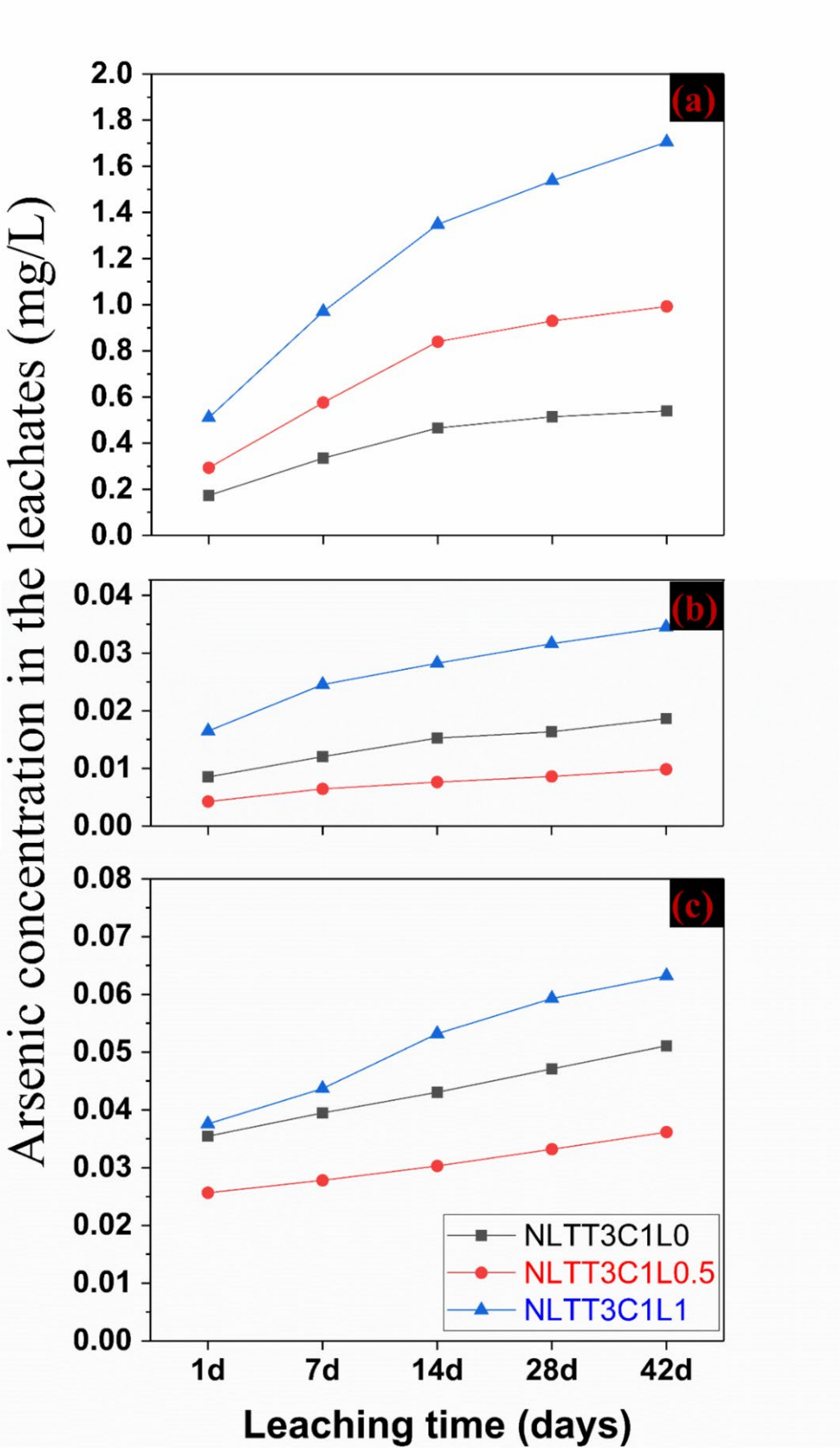

Figure 9. Leachability of As from concrete bricks using different leachants: (a) 0.1M NaOH, (b) distilled water, and (c) 0.1M HCl

During the 42 days leaching trial, the pH of the leachates in 0.1 M NaOH, HNO_3, and distilled water were 12–13, 1–3, and 10–11, respectively. The reduction of pH of acid leachate and increase of pH of alkali leachate is expected because they are consistent with the pH of the leachants. The increase of pH of the distilled water (pH around 7) leachate is due to the dissolution of calcium (Ca) hydroxide present in cement and added lime. A similar increase in pH of water leachate from concrete bricks was reported by Nguyen et al. (2020b). An increase of leachate pH and the presence of Ca in concrete and added lime would have resulted in the formation of Ca-As precipitates (calcium arsenate, calcium arsenite, calcium hydrogen arsenate hydrate, and calcium hydrogen arsenate), and this might have reduced the concentration of As in the leachate (Jing et al., 2005; Silva et al., 2019).

.

4. Conclusions

A new type of household filtration system packed with 15 kg of low-cost NLTT was designed and successfully operated to remove As(V) from groundwater after a pre-treatment with the existing traditional sand filtration at four sites in two communes in Ha Nam province and Hanoi, Vietnam. This filter system was able to produce safe drinking water continuously for seven months with As level below the WHO and Vietnam drinking water limits. Laboratory column study with NLTT indicated that the breakthrough curves fitted the Thomas model very satisfactorily with adsorption capacities of 0.06 and 0.20 mg/g at a flow velocity of 0.85 m/h for the influent As(V) concentrations of 0.1 and 0.5 mg/L, respectively. Spent adsorbent waste could be managed through the solidification/stabilization technique to prevent As being released to the environment. The mass ratio of As solid waste: Portland cement: lime of 3: 1: 0.5 was determined to be a favourable ratio for producing good concrete bricks that also restrain the mobility of As. The concrete bricks had acceptable compressive strength for use as a building material in construction work.

Acknowledgement

This study was financially supported by the Aus4Innovation program – a development cooperation initiative funded by the Australian Department of Foreign Affairs and Trade and InnovationXchange, and managed by the Commonwealth Scientific and Industrial Research Organization, in partnership with the Ministry of Science and Technology of Vietnam. The first author thanks University of Technology Sydney for a PhD studentship.

REFERENCES

QCVN 01:2009/BYT. National Technical Regulation on Drinking Water Quality. Department of Preventive Medicine & Environment and Promulgated by Ministry of Health's minister.

Abdolali, A., Ngo, H. H., Guo, W., Zhou, J. L., Zhang, J., Liang, S., Chang, S. W., Nguyen, D. D., Liu, Y., 2017. Application of a breakthrough biosorbent for removing heavy metals from synthetic and real wastewaters in a lab-scale continuous fixed-bed column. Bioresource Technology 229, 78-87.

Agusa, T., Kunito, T., Fujihara, J., Kubota, R., Minh, T. B., Trang, P. T. K., Iwata, H., Subramanian, A., Viet, P. H., Tanabe, S., 2006. Contamination by arsenic and other trace elements in tube-well water and its risk assessment to humans in Hanoi, Vietnam. Environmental Pollution 139, 95-106.

Ali, I., 2018. Microwave assisted economic synthesis of multi walled carbon nanotubes for arsenic species removal in water: batch and column operations. Journal of Molecular Liquids 271, 677-685.

Asif, Z., Chen, Z., 2017. Removal of arsenic from drinking water using rice husk. Applied Water Science 7, 1449-1458.

Berg, M., Stengel, C., Trang, P. T. K., Viet, P. H., Sampson, M. L., Leng, M., Samreth, S., Fredericks, D., 2007. Magnitude of arsenic pollution in the Mekong and Red River Deltas—Cambodia and Vietnam. Science of the Total Environment 372, 413-425.

Berg, M., Tran, H. C., Nguyen, T. C., Pham, H. V., Schertenleib, R., Giger, W., 2001. Arsenic contamination of groundwater and drinking water in Vietnam: a human health threat. Environmental Science & Technology 35, 2621-2626.

Brandhuber, P., Amy, G., 1998. Alternative methods for membrane filtration of arsenic from drinking water. Desalination 117, 1-10.

Brion-Roby, R., Gagnon, J., Deschênes, J.-S., Chabot, B., 2018. Investigation of fixed bed adsorption column operation parameters using a chitosan material for treatment of arsenate contaminated water. Journal of Environmental Chemical Engineering 6, 505-511.

Cheng, Y., Zhang, S., Huang, T., Li, Y., 2019. Arsenite removal from groundwater by iron–manganese oxides filter media: Behavior and mechanism. Water Environment Research 91, 536-545.

Eeshwarasinghe, D., Loganathan, P., Kalaruban, M., Sounthararajah, D. P., Kandasamy, J., Vigneswaran, S., 2018. Removing polycyclic aromatic hydrocarbons from water using granular activated carbon: kinetic and equilibrium adsorption studies. Environmental Science and Pollution Research 25, 13511-13524.

Glocheux, Y., Pasarín, M. M., Albadarin, A. B., Allen, S. J., Walker, G. M., 2013. Removal of arsenic from groundwater by adsorption onto an acidified laterite by-product. Chemical Engineering Journal 228, 565-574.

Glodowska, M., Stopelli, E., Straub, D., Thi, D. V., Trang, P. T., Viet, P. H., Berg, M., Kappler, A., Kleindienst, S., 2021. Arsenic behavior in groundwater in Hanoi (Vietnam) influenced by a complex biogeochemical network of iron, methane, and sulfur cycling. Journal of Hazardous Materials 407, 124398.

Goh, K.-H., Lim, T.-T., Dong, Z., 2008. Application of layered double hydroxides for removal of oxyanions: a review. Water Research 42, 1343-1368.

Jing, C., Liu, S., Meng, X., 2005. Arsenic leachability and speciation in cement immobilized water treatment sludge. Chemosphere 59, 1241-1247.

Kalaruban, M., Loganathan, P., Nguyen, T. V., Nur, T., Johir, M. A. H., Nguyen, T. H., Trinh, M. V., Vigneswaran, S., 2019. Iron-impregnated granular activated carbon for arsenic removal: application to practical column filters. Journal of Environmental Management 239, 235-243.

Kim, K.-W., Chanpiwat, P., Hanh, H. T., Phan, K., Sthiannopkao, S., 2011. Arsenic geochemistry of groundwater in Southeast Asia. Frontiers of Medicine 5, 420-433.

Kofa, G., NdiKoungou, S., Kayem, G., Kamga, R., 2015. Adsorption of arsenic by natural pozzolan in a fixed bed: determination of operating conditions and modeling. Journal of Water Process Engineering 6, 166-173.

Kundu, S., Gupta, A., 2008. Immobilization and leaching characteristics of arsenic from cement and/or lime solidified/stabilized spent adsorbent containing arsenic. Journal of Hazardous Materials 153, 434-443.

Lata, S., Samadder, S., 2016. Removal of arsenic from water using nano adsorbents and challenges: a review. Journal of Environmental Management 166, 387-406.

Lievremont, D., Bertin, P. N., Lett, M.-C., 2009. Arsenic in contaminated waters: biogeochemical cycle, microbial metabolism and biotreatment processes. Biochimie 91, 1229-1237.

Meng, X., Korfiatis, G. P., 2001. Removal of arsenic from Bangladesh well water using a household filtration system, BUETUNU International Workshop on Technologies for Arsenic Removal from Drinking Water, Dhaka, Bangladesh.

Mohan, D., Pittman Jr, C. U., 2007. Arsenic removal from water/wastewater using adsorbents—a critical review. Journal of Hazardous Materials 142, 1-53.

Nguyen, T., Ngo, H., Guo, W., Pham, T., Li, F., Nguyen, T., Bui, X., 2015. Adsorption of phosphate from aqueous solutions and sewage using zirconium loaded okara (ZLO): fixed-bed column study. Science of the Total Environment 523, 40-49.

Nguyen, T. H., Tran, H. N., Vu, H. A., Trinh, M. V., Nguyen, T. V., Loganathan, P., Vigneswaran, S., Nguyen, T. M., Vu, D. L., Nguyen, T. H. H., 2020a. Laterite as a low-cost adsorbent in a sustainable decentralized filtration system to remove arsenic from groundwater in Vietnam. Science of The Total Environment 699, 134267.

Nguyen, T. T. Q., Loganathan, P., Nguyen, T. V., Vigneswaran, S., 2020b. Removing arsenate from water using modified manganese oxide ore: Column adsorption and waste management. Journal of Environmental Chemical Engineering 8, 104491.

Nguyen, T. T. Q., Loganathan, P., Nguyen, T. V., Vigneswaran, S., 2020c. Removing arsenic from water with an original and modified natural manganese oxide ore: batch kinetic and equilibrium adsorption studies. Environmental Science and Pollution Research 27, 5490-5502.

Nguyen, T. V., Nguyen, T. V. T., Pham, T. L., Vigneswaran, S., Ngo, H. H., Kandasamy, J., Nguyen, H. K., Nguyen, D. T., 2009. Adsorption and removal of arsenic from water by iron ore mining waste. Water Science and Technology 60, 2301-2308.

Nitzsche, K. S., Lan, V. M., Trang, P. T. K., Viet, P. H., Berg, M., Voegelin, A., Planer-Friedrich, B., Zahoransky, J., Müller, S.-K., Byrne, J. M., 2015. Arsenic removal from drinking water by a household sand filter in Vietnam—Effect of filter usage practices on arsenic removal efficiency and microbiological water quality. Science of the Total Environment 502, 526-536.

Nur, T., Shim, W., Loganathan, P., Vigneswaran, S., Kandasamy, J., 2015. Nitrate removal using Purolite A520E ion exchange resin: batch and fixed-bed column adsorption modelling. International Journal of Environmental Science and Technology 12, 1311-1320.

Pena, M. E., Korfiatis, G. P., Patel, M., Lippincott, L., Meng, X., 2005. Adsorption of As (V) and As (III) by nanocrystalline titanium dioxide. Water Research 39, 2327-2337.

Rout, P. R., Bhunia, P., Dash, R. R., 2015. A mechanistic approach to evaluate the effectiveness of red soil as a natural adsorbent for phosphate removal from wastewater. Desalination and Water Treatment 54, 358-373.

Roy, P., Mondal, N. K., Bhattacharya, S., Das, B., Das, K., 2013. Removal of arsenic (III) and arsenic (V) on chemically modified low-cost adsorbent: batch and column operations. Applied Water Science 3, 293-309.

Shaji, E., Santosh, M., Sarath, K., Prakash, P., Deepchand, V., Divya, B., 2020. Arsenic contamination of groundwater: A global synopsis with focus on the Indian Peninsula. Geoscience Frontiers.

Siddiqui, S. I., Chaudhry, S. A., 2017. Iron oxide and its modified forms as an adsorbent for arsenic removal: A comprehensive recent advancement. Process Safety and Environmental Protection 111, 592-626.

Silva, L. C., Neves, V. A., Ramos, V. S., Silva, R. S., Campos, J. B. d., Silva, A. A. d., Malta, L. F., Senra, J. D., 2019. Layered double hydroxides as bifunctional catalysts for the aryl borylation under ligand-free conditions. Catalysts 9, 302.

Singh, T. S., Pant, K., 2006. Solidification/stabilization of arsenic containing solid wastes using portland cement, fly ash and polymeric materials. Journal of Hazardous Materials 131, 29-36.

Smedley, P. L., Kinniburgh, D. G., 2002. A review of the source, behaviour and distribution of arsenic in natural waters. Applied Geochemistry 17, 517-568.

Sullivan, C., Tyrer, M., Cheeseman, C. R., Graham, N. J., 2010. Disposal of water treatment wastes containing arsenic—a review. Science of the Total Environment 408, 1770-1778.

Te, B., Wichitsathian, B., Yossapol, C., Wonglertarak, W., 2018. Investigation of arsenic removal from water by iron-mixed mesoporous pellet in a continuous fixed-bed column. Water, Air, & Soil Pollution 229, 1-15.

Thomas, H. C., 1944. Heterogeneous ion exchange in a flowing system. Journal of the American Chemical Society 66, 1664-1666.

WHO, 1993. Guidelines for Drinking-water Quality.

Yunnen, C., Ye, W., Chen, L., Lin, G., Jinxia, N., Rushan, R., 2017. Continuous Fixed-Bed Column Study and Adsorption Modeling: Removal of Arsenate and Arsenite in Aqueous Solution by Organic Modified Spent Grains. Polish Journal of Environmental Studies 26.

Zhao, Z., Guan, M., Zeng, H., Chen, P., 2018. Adsorption and Oxidation of As (III) on Iron (Hydro) Oxides: Zhao et al. Water Environment Research 90, 483-489.